Original Article

Bulletin of Pure and Applied Sciences.
Vol.37 C (Chemistry), No.1, 2018: P.36-42
Print version ISSN 0970 4620
Online version ISSN 2320 320X
DOI 10.5958/2320-320X.2018.00006.7

Photocatalytic degradation of an acidic dye and a basic dye using heterostructured photocatalyst

Baiju V[1,*], Dedhila Devadathan[1], Raveendran R[1]

Author Affiliations
[1]Nanoscience Research Laboratory, Department of Physics, Sree Narayana College, Kollam, 691001, Kerala.

Corresponding Author
*__Baiju V,__ Nanoscience Research Laboratory, Department of Physics, Sree Narayana College, Kollam, 691001, Kerala.

E-mail: baijuvkollam@gmail.com

Received on 15th January 2018
Accepted on 30th January 2018

Abstract

Most of the natural resources of drinking water are found to be contaminated with various toxic materials. One of the most relevant pollutants is organic dyes. Photocatalysis is a promising green technology for the removal of dyes. In the present work heterostructured NiO/ZnO nanocomposite was prepared using co–precipitation method, analyzed using XRD, SEM and UV/Vis spectroscopy. For comparison purpose NiO was also prepared. Comparison of XRD's of metal oxides with JCPDS confirmed the formation of heterojunctions. UV/Vis absorption studies confirmed the shift of the optical absorption towards the visible region. The photocatalytic degradations of dyes namely Malachite Green, a basic and Congo Red, an acidic dye were carried out using the prepared composite. Factors affecting photocatalytic degradation like effect of contact time, amount of photocatalyst and dye concentration were also investigated. Results suggested an increase in degradation efficiency in the case of heterojunctions nanocomposite as compared to individual metal oxide.

Keywords: Photocatalysis, Heterojunction, Nanocomposite, Photocatalyst, Co–precipitation

1. INTRODUCTION

Nature has its own mechanism for water recycling to provide us with sufficient quantity of fresh water with consumable purity level. Modern human activities have however disrupted the balance between the usage and natural purification process, leading to a shortage of potable water. Most of the natural resources of drinking water are found to be contaminated with various toxic materials and pathogenic microorganisms. One of the most relevant pollutants is organic dyes. The dyes have diverse applications in various industries of paper, leather, cosmetics, drugs, electronics, plastics and printing and approximately 80% of the synthetic dyes are consumed by the textile industry. Dyes are non biodegradable compounds and human exposure to wastewater which contains dyes is highly dangerous and these carcinogenic compounds show high resistance against biological, physical and

chemical reactions. Many researchers consider advanced oxidation process as the most effective, economically feasible and applicable technology for the removal of organic dye pollutants. Nanotechnology is widely applied for purification and treatment of waste water. The novel properties of nanomaterials such as large surface area, potential for self assembly, high specificity, high reactivity and catalytic potential make them excellent candidates for this application. An expanding trend for the nanomaterials is the fabrication of composite structures with materials capable of enhancing the properties. Many efforts have been made for the synthesis of different coupled semiconductors [1–4]. The synthesized coupled semiconductors significantly improve the photocatalytic efficiency by decreasing the recombination rate of the photogenerated electron–hole pairs and present potential application in water splitting, organic decomposition and photovoltaic device [5]. In the present study heterojuction NiO/ZnO nanocomposite is prepared and applied as photocatalyst.

2. MATERIALS AND METHODS

AR grade chemicals obtained from Merck were used for the preparation of NiO/ZnO heterojunction. NiO (NF) and NiO/ZnO (NZF) were prepared by the co–precipitation method in presence of capping agent. NF and NZF annealed at 5000c for three hours, was used for analysis. XRD studies were carried out using XPERT–PRO model powder diffractometer (PAN analytical, Netherlands) employing Cu–Kα radiation (λ = 1.54060Ao) operating at 40kV, 30mA. SEM of the samples was obtained using JEOL/EO Model JSM–6390LV scanning electron microscope. The absorbance spectra, reflectance spectra and photocatalysis studies of the sample was studied using JASCO V 650, UV/Vis spectrophotomer.

Metal oxides prepared in the present study were obtained in the form of hydroxides. The nickel hydroxide was obtained as dark green powder where as in the case of NiO/ZnO was obtained as light pista green powders. But both the annealed samples were black in colour.

3. RESULTS AND DISCUSSION

X–ray diffractograms of NF and NZF is shown in Figure 1. The well defined X–ray diffraction peaks in the case of NF and NZF indicate that NiO and NiO/ZnO formed are crystalline in nature. Also, the diffraction peaks are notably broadened indicating the smaller crystallite size. In order to confirm the phase purity of the samples prepared, the interplanar spacing (dhkl values), 2θ values and relative intensity values corresponding to the observed diffraction peaks were compared with the standard values of NiO in case of NF and in case of NZF the observed diffraction peaks were compared with the standard values of NiO and ZnO as reported by JCPDS–International Centre for Diffraction Data.

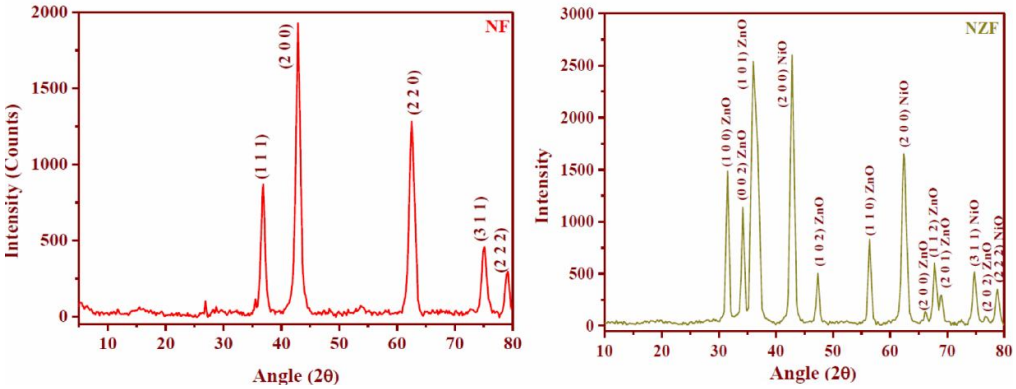

Fig. 2: XRD Spectrum of NF and NZF

XRD pattern for ZnO prepared using the very same procedure in our lab was used for JCPDS comparison in case of ZnO [6]. The obtained pattern for ZnO was found to match well with JCPDS–ICDD pattern number #79–0205. From the comparison of diffraction peaks NF with JCPDS–ICDD pattern number #78–0423 it is clear that NiO formed was a cubic system with FCC lattice. The data obtained for NiO/ZnO matched with JCPDS–ICDD pattern number #78–0423 of NiO and JCPDS–ICDD pattern number #79–0205 of ZnO separately. From JCPDS, NiO shows cubic system with FCC lattice and ZnO shows hexagonal system with primitive lattice. The variation observed in the d values of the crystal planes in case of NZF when compared to NiO and ZnO, confirms the formation of composites. This is also supported by the disappearance of the peak corresponding to (1 0 3) of ZnO in the XRD of the nanocomposite. The average crystallite size was calculated from the line broadening of the XRD pattern, making use of Scherrer formula. The crystallite size calculated using FWHM (Full width at half maximum) values of five major peaks in the XRD spectrum of NF using Scherrer equation are shown in the Table 1. In case of NZF the average crystallite size of NZF calculated from the line broadening of the XRD pattern, using FWHM values of seven major peaks in the XRD spectrum making use of Scherrer formula are shown in Table 2.

Table 1: Crystallite size calculation of NF using Scherrer equation

2θ	θ	Cosθ	FWHM	D (nm)
36.845	18.42	0.9488	0.719	11.65
42.873	21.44	0.9309	0.774	11.03
62.518	31.26	0.8549	0.858	10.84
75.075	37.54	0.7932	0.914	10.96

Average Crystallite size = 11.12± 0.3 nm

Table 2: Crystallite size calculation of NS using Scherrer equation

2θ	θ	Cosθ	FWHM	D (nm)
31.54	15.77	0.9624	0.383	21.56
34.20	17.10	0.9558	0.397	20.95
36.04	18.02	0.9509	0.353	23.67
42.85	21.42	0.9309	0.577	14.79
47.34	23.67	0.9159	0.459	18.91
56.41	28.20	0.8814	0.460	19.60
62.44	31.22	0.8553	0.801	11.60

Average Crystallite size = 18.73± 3 nm

The SEM images of NF and NZF are shown in Figure 2. NF showed agglomeration of spherical particles or cauliflower like morholopgy and NZF showed agglomeration of very small spherical particles of almost simlar uniform dimensions.

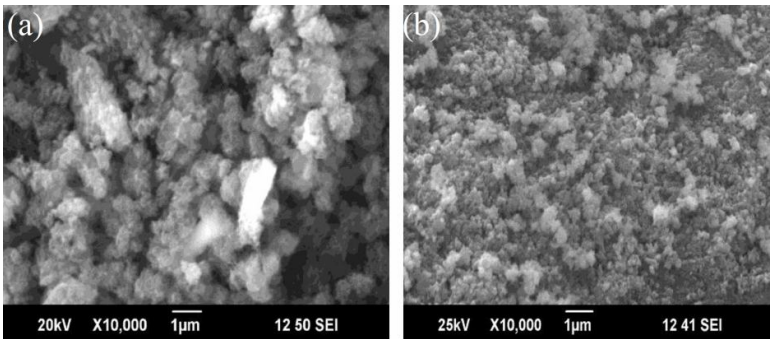

Fig. 2: SEM images of (a) NF and (b) NZF

The UV–Vis absorption spectrum of the NF taken in the wavelength range 210 to 850 nm with 1 nm resolution is shown in the Figure 3. Presence of an absorption band is observed in the range 225 nm – 270 nm with λ_{max} situated at 249nm in case of NF.

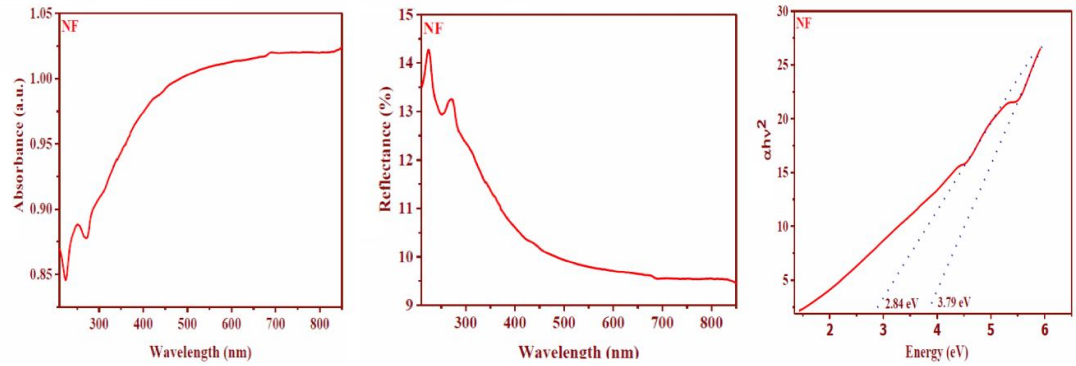

Fig. 3: UV/VisAbsorbance, Reflectance spectra and Tauc Plot of NF

An additional absorption band is observed in the wavelength range 270 nm – 305 nm. It is reported in literature that optical energy band gap of NiO lies in the range (3.6–4.0 eV) [Adler and Feinleib, 1970] and is attributed to charge–transfer transition between the valence bands of O (p) states to conduction bands of Ni d (e_{2g}) states [7]. The absorption edge is found to be 4.98 eV for NF. Figure 3 also shows the reflectance spectrum obtained for NF. The percentage reflectance corresponding to λ_{max} situated at 249 nm was found to be 12.94 %.

The materials also showed sub band gaps. This might be due to d–d transitions. The optical band gap of NF determined from the absorption spectra using Tauc's relation were 2.84 eV and 3.79 eV. Tauc's plot drawn for NF is also shown in Figure 3.

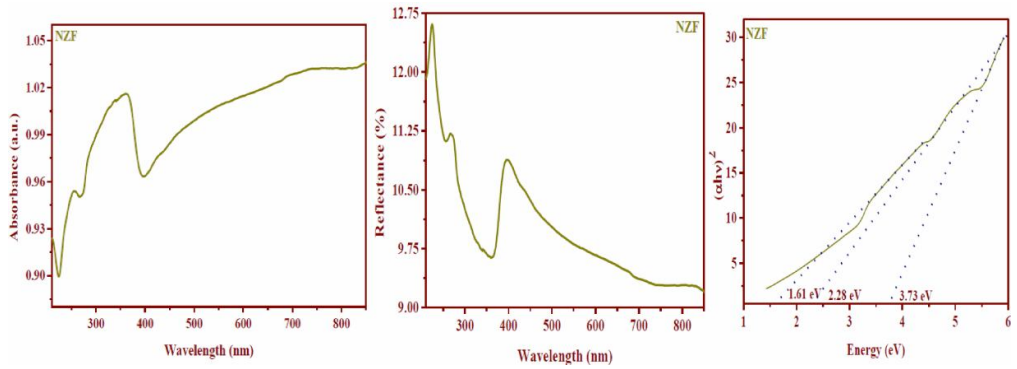

Fig. 4: UV/Vis Absorbance, Reflectance spectra and Tauc Plot of NZF

The UV–Vis absorption and reflectance spectra of NZF taken in the wavelength range 210 to 870 nm with 1 nm resolution is shown in the Figure 4. Presence of a weak absorption band was observed in the range 225 nm – 270 nm with λ_{max} situated at 256nm and also another strong absorption band in the range 260 nm – 400 nm with λ_{max} situated at 360 nm was also obtained. The shift of peak from 252 nm of NF to 256 nm in NZF can be attributed to the interaction between NiO and ZnO. The second band can be attributed to the presence of ZnO which could be assigned to the intrinsic band–gap absorption of ZnO due to the electron transitions from the valence band to the conduction band ($O_{2p} \rightarrow Zn_{3d}$) [8]. The absorption edge was found to be 3.44 eV for NZF. Figure 4 also shows the

reflectance spectrum obtained for NZF. The percentage reflectance corresponding to λmax values for NZF were found to be 9.6%. The optical band gap determined from the absorption spectra using Tauc's relation for NZF is shown in Figure 4.

Surface area and surface defects play an important role in photocatalytic efficiency and many other practical properties. In the present work the nanocomposite showed good visible light absorption in addition to UV absorption. Hence proper tuning could make these nanocomposites excellent candidates for many practical applications such as anti–bacterial, deodorizing, air purifying, anti fogging and as other surface purification agents.

The prepared sample was used as photocatalyst for the degradation of Malachite Green, and Congo Red. Organic dyes of 1000 ppm concentration were prepared and the desired concentrations were taken and used as dye samples. The photocatalytic activity of samples for the degradation of the dyes; Congo red (CR) and Malachite green (MG) and were studied using the respective photocatalyst in the presence of UV illumination in a photoreactor. The experiments were performed by suspending the desired amount of photocatalyst into 300 ml of dye solution of desired concentration which was varied from 25 ppm to 75 ppm. The experiment was carried out isothermally at 300 K. The concentration of residual dye in the solution after irradiation for 2 hrs was determined by monitoring the absorbance intensity of solution samples at their maximum absorbance wavelength by using UV–Vis spectrophotometer (JASCO V 650 UV–Vis spectrophotometer). In the present work various factors affecting photocatalytic degradation like effect of contact time, amount of photocatalyst and dye concentration were also investigated. To study the effect of contact time on the photodegradation of organic dyes, the following procedure was adopted. To the respective dye solution of concentration, 25 ppm in 300 ml solution kept at 300 K, 0.1 g of the photocatalyst was added and was kept under UV light. After desired time intervals [30, 60, 90 and 120 min], 10 mL of the solution was taken out, centrifuged and UV–Vis absorption spectra was recorded. In the above experiment, the amount of photocatalyst was varied from 0.025g to 0.125g to study its effect on photodegradation. Dye solutions of three different concentrations were selected (25 ppm, 50 ppm and 75 ppm) to study the effect of initial dye concentration on photodegradation efficiency.

The photocatalytic degradation efficiency was calculated as follows:

$$\text{Photocatalytic degradation efficiency (\%)} = \frac{(C_0 - C_t)}{C_0} \times 100 \quad \cdots\cdots(1)$$

C_0: initial concentration of dye solution [mgL–1],
C_t: final concentration of dye solution [mgL–1],

In the present work NiO/ZnO composites prepared are coupled heterogeneous system. When NiO/ZnO coupled metal oxide is irradiated by visible light, the electrons in the valence band (VB) of ZnO and NiO are excited to their conduction bands (CB) or to the defect levels present in the band gap. The excited electrons from CB of NiO are transferred to the low lying CB of ZnO. The holes are transferred from the VB of ZnO to the VB of NiO. This in turn leads to the efficient separation of photogenerated electron–hole pairs. As a result, the photocatalytic activity of the NiO/ZnO coupled metal oxide is significantly enhanced. The efficient visible light photocatalytic degradation shown by the coupled metal oxides could be due to the stoichiometry deficiency induced on coupling and the formation of defect energy levels. Figure 5 shows the suggested mechanism in the case of photocatalytic degradation process using NiO/ZnO. In contrast to single phase photocatalysts, heterojunction semiconductors or integrated multi–semiconductor systems possess significant advantages in promoting the separation of electron–hole pairs and keeping reduction and oxidation reactions of photocatalysis at two different reaction sites. Formation of heterojunction greatly diminishes the electron–hole pairs recombination and increases the life time of charge carriers, thus promoting the photocatalytic efficiency. A schematic diagram of the mechanism of photocatalysis is given below.

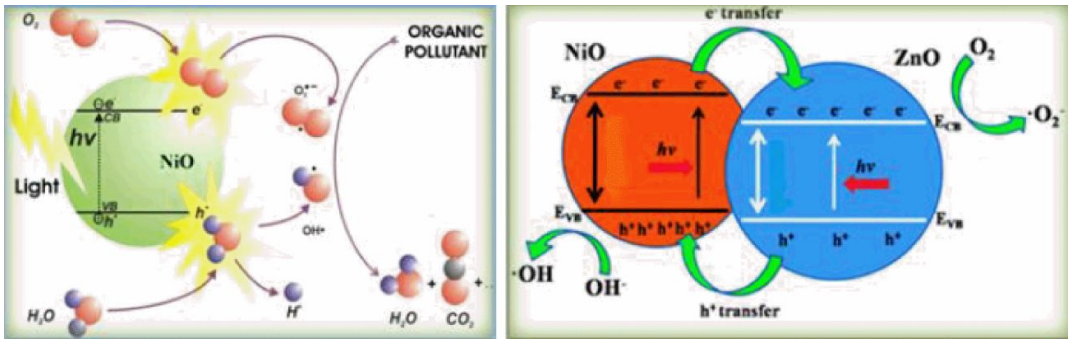

Fig. 5: Mechanism of Photocatalytic degradation process using NiO and NiO/ZnO hetrojunction nanocomposite

The percentage of photodegradation increased with increase in contact time of the dye and the catalyst. The amount of catalyst loading is one of the main parameters for the degradation efficiency. In order to avoid the use of excess catalyst it is necessary to find out the optimum loading for efficient removal of dye. The results showed that when catalyst dosage was increased from 0.025 to 0.075 g, the percentage de–colorization increased. However, on further increase in dosage of the catalyst beyond 0.1 g, there was a slight decrease in the degradation percentage. In the absence of photocatalyst it was found that CR dye is difficult to be oxidized by only UV light. The increase in degradation rate with increase in the catalyst loading is due to increase in total active surface area i.e. availability of more active sites on catalyst surface [9]. However, it increases significantly upon addition of photocatalyst due to the generation of higher amount of hydroxyl radical through the interaction of UV light with photocatalyst. But above 0.1 g, the percentage degradation significantly decreased due to decrease of formation of hydroxyl radicals. It should be pointed out that, the catalyst loading affects both the number of active sites on photocatalysts and the penetration of UV light through the suspension [10]. With increasing catalyst loading the number of active sites increases, but the penetration of UV light decreases due to shielding effect [11]. It should also be noted that the optimum value of catalyst loading is strongly dependent on the type and initial concentration of the dye and the operating conditions of the photoreactor [12]. The optimum concentration of the catalyst for efficient UV photodecolorization and degradation was found to be 0.1 g/300ml.

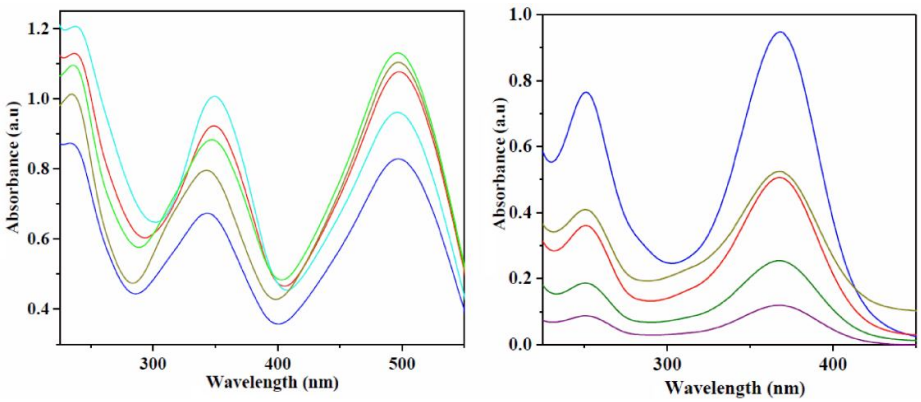

Fig. 6: Photocatalytic degradation of CR and MG

The rate of photocatalytic degradation decreased with the increasing initial dye concentration. As the initial concentration of a dye increases, the colour of dye solution becomes deeper which results in less penetration of light to the surface of the catalyst, decreasing the number of excited dye molecules. With increase in initial concentration of dye more and more organic substances are adsorbed on the surface of the photocatalyst. Therefore, the generation of hydroxyl radicals is reduced, since there are only fewer active sites in the system [13]. Similar results have been reported by other researchers for

the photocatalytic oxidation of pollutants [9]. The activity of the nanocomposite was also compared with the counterpart.

4. CONCLUSIONS

It was observed from the UV/Vis spectral analysis that the nanocomposites showed absorption in visible range in addition to UV light. Hence these materials could be used as photocatalyst in the degradation of organic dyes under solar ray irradiation. Results suggested an increase in degradation efficiency in the case of heterojunction nanocomposite when compared to metal oxide. It is suggested that these materials could be efficiently used as anti–bacterial, deodorizing, air purifying, anti fogging and as other surface purification agents.

Acknowledgements

We acknowledge STIC, Cochin, Kerala for Sample analysis.

REFERENCES

[1] Bessekhouad Y, Robert D and Weber J V, J. Photochem.Photobiol., A: Chemistry, **2004**.
[2] Shifu C, Lei C, Shen G and Gengyu C, Mater. Chem. Phys., 98, **2006**, 116–120.
[3] Wang C, Zhao J, Wang X, Mai B, Sheng G, Peng P and Fu J, Appl. Catal. B: Environ., 39, **2002**, 269–279.
[4] Zhang S. et.al. Journal of Alloys and Compounds, 426, **2006**, 281–285.
[5] Kamat P V, J. Phys. Chem. C, 112, **2008**, 18737–18753.
[6] Dedhila D and Raveendran R, International Journal of Chemical Engineering and Applications, 5, **2014**, 240–243.
[7] Lenglet M, Hochu F, Durr J and Tuilier MH, Solid State Commun.,104, **1997**,793–798.
[8] Haldorai Y, Chitra S and Shim J J, Advanced Science, Engineering and Medicine 5, 2013, 1–7.
[9] Goncalves MST et.al. Chemosphere, 39, **1999**, 781–786.
[10] Daneshvar N, Salari D and Khataee A R, J. Photochem, Photobiol. A. Chem., 157, **2003**, 111–116.
[11] Gouvea CAK, Wypych F, Moraes SG, Durán N and Peralta– Zamora P, Chemosphere, 40, **2000**, 433–440.
[12] Gogate P R and Pandit A B, Adv. Environ. Res., 8, **2004**, 553–597.
[13] Daneshvar N, Salari D and Khataee A R, J. Photochem. Photobiol., A: Chem., 162, **2004**, 317–322.